The final version of this article was published in

PHYSICAL REVIEW B 84(8) 085140 (2011)

DOI: 10.1103/PhysRevB.84.085140

Luminescence and x-ray absorption measurements of persistent $SrAl_2O_4$:Eu,Dy powders: Evidence for valence state changes

K. Korthout[1], K. Van den Eeckhout[1], J. Botterman[1], S. Nikitenko[2], D. Poelman[1], and P. F. Smet[1,*]

[1]LumiLab, Dept. Solid State Sciences, Ghent University, Krijgslaan 281-S1, 9000 Gent, Belgium
[2]Netherlands Organisation for Scientific Research (NWO), DUBBLE at ESRF, BP220, 38043 Grenoble CEDEX 9, France

*corresponding author: philippe.smet@ugent.be

The development of new efficient afterglow phosphors is currently hampered by a limited understanding of the persistent luminescence mechanism. Radioluminescence and x-ray absorption measurements on the persistent phosphor $SrAl_2O_4$:Eu,Dy were combined to reveal possible valence state changes for the rare earth (co)dopants. Traps in the phosphor material are quickly filled when exposing thermally emptied $SrAl_2O_4$:Eu,Dy powder to x-rays. On the same time scale, a partial oxidation of Eu^{2+} to Eu^{3+} is observed by XANES (x-ray absorption near-edge spectroscopy), while for the trivalent dysprosium the valence state remains unchanged. The impact of these observations on the recently proposed models for persistent luminescence is discussed.

Luminescence and x-ray absorption measurements of persistent $SrAl_2O_4$:Eu,Dy powders: Evidence for valence state changes

K. Korthout[1], K. Van den Eeckhout[1], J. Botterman[1], S. Nikitenko[2], D. Poelman[1], and P. F. Smet[1,*]

[1]LumiLab, Dept. Solid State Sciences, Ghent University, Krijgslaan 281-S1, 9000 Gent, Belgium
[2]Netherlands Organisation for Scientific Research (NWO), DUBBLE at ESRF, BP220, 38043 Grenoble CEDEX 9, France

*corresponding author: philippe.smet@ugent.be

The development of new efficient afterglow phosphors is currently hampered by a limited understanding of the persistent luminescence mechanism. Radioluminescence and x-ray absorption measurements on the persistent phosphor $SrAl_2O_4$:Eu,Dy were combined to reveal possible valence state changes for the rare earth (co)dopants. Traps in the phosphor material are quickly filled when exposing thermally emptied $SrAl_2O_4$:Eu,Dy powder to x-rays. On the same time scale, a partial oxidation of Eu^{2+} to Eu^{3+} is observed by XANES (x-ray absorption near-edge spectroscopy), while for the trivalent dysprosium the valence state remains unchanged. The impact of these observations on the recently proposed models for persistent luminescence is discussed.

I. Introduction

Some photoluminescent materials are able to continue emitting light for minutes or hours after the excitation has ended, a phenomenon known as persistent luminescence. Although such materials have been reported as early as 1602[1], it was only in 1996 that this field of research started to attract wider interest due to the discovery of the very bright and long-lasting afterglow of $SrAl_2O_4$:Eu,Dy by Matsuzawa *et al.* [2]. Since then, several other persistent luminescent materials have been developed[1], mainly aluminates and silicates, but up to now $SrAl_2O_4$:Eu,Dy remains the most important and most studied afterglow phosphor. It has a bright green afterglow which remains visible for over 30 hours to the dark-adapted eye. Currently, persistent luminescent materials are mainly applied in emergency lighting, safety signage and bio-imaging[1,3,4]. However, the development of new materials with different properties and emission colors is expected to allow a new range of applications.

Despite these fifteen years of intensive research, the mechanism behind the persistent luminescence phenomenon is not yet fully resolved. Most authors agree on the general idea that charge carriers are created inside the material, which subsequently get trapped by long-lived energy levels inside the forbidden zone of the host crystal. However, the nature of these traps and the type and origin of the trapped carriers remains the subject of debate, although several structural and optical analytical techniques (such as x-ray absorption spectroscopy [5,6], electron spin resonance [7], photoconductivity measurements [8] and thermoluminescence spectroscopy [9]) have been applied to a wide range of persistent phosphors. Often, rare earth codopants considerably enhance the afterglow, but also several non-codoped persistent phosphors have been reported [2,10]. For example, $SrAl_2O_4$:Eu has a considerable afterglow of around 1 hour, indicating that the presence of Dy ions in the host is not imperative. Many of the models that were developed in recent years predict the release of electrons by ionization of photo-excited Eu^{2+}-ions to Eu^{3+}. The hereby liberated electrons are then supposedly

trapped by the rare earth codopants (Dorenbos[11]), neighboring crystal vacancies (Clabau et al.[12]) or both (Aitasalo et al.[13]).

We have performed a series of x-ray absorption spectroscopy (XAS) experiments on the Eu and Dy L_{III}-edges of $SrAl_2O_4$:Eu,Dy, combined with in-situ radioluminescence (RL) studies, with a double goal. Firstly, we want to demonstrate that XAS can be an interesting technique to study valence states in persistent phosphors on condition the experiments are carefully conducted. Secondly, we will show that a valence state change upon filling the traps in $SrAl_2O_4$:Eu,Dy occurs for the dopant (Eu), but not for the co-dopant (Dy). Valence state changes of lanthanide ions were already observed in other systems in real time using XAS. Moreau et al. investigated the valence state changes of europium in aqueous and non-aqueous systems upon exposure to oxygen [14, 15]. Martin et al. recorded valence state changes of samarium in $Sm_{0.75}Y_{0.25}S$ upon heating of the sample from 77K to 300K [16].

II. Experimental setup

The XAS measurements were carried out at the Dutch-Belgian beam line (DUBBLE, BM26A) of the 6 GeV European Synchrotron Radiation Facility (ESRF) in Grenoble, France operating with a 160-200 mA electron current[17]. RL was used to investigate the charging behavior of the phosphor under X-ray irradiation, while X-ray absorption near-edge structure (XANES) spectra were collected to study the presence and valence of Eu and Dy in the sample during the charging process.

The sample powder (GloTech Intl.[18]) was put in 2mm diameter quartz capillaries (wall thickness of 10µm) and heated on a hot plate before each experiment well beyond the thermoluminescent glow peak. In this way, we can assume that all relevant traps are completely emptied at the start of each experiment. During the X-ray irradiation, the material was kept at 120K (+/- 20K) using an Oxford 700 series Cryostream. RL data were collected with an OceanOptics QE65000 spectrometer, covering the entire visible spectrum, with a frame rate of 500ms. Samples were mounted without exposure to ambient light and during the x-ray irradiation the sample environment was kept dark.

The synchrotron radiation was monochromated with a double Si(111) monochromator, suppressing the higher harmonics. EuS, Eu_2O_3 and Dy_2O_3 were used as energy reference materials. Eu L_{III}–edge and Dy L_{III}-edge XANES spectra were recorded in the energy range 6.78-7.03 keV and 7.75-7.84 keV respectively with an energy step of typically 0.85 eV. XANES spectra for the reference materials were collected in transmission mode using ion chambers. The XANES spectra of $SrAl_2O_4$:Eu,Dy were collected in fluorescence mode (Fig. 1) by monitoring the Eu and Dy $L\alpha_1$ peak fluorescence lines (centered around 5.85 and 6.50 keV, respectively). The $SrAl_2O_4$:Eu,Dy phosphors could not be measured in transmission mode because of the low dopant concentration and the relatively strong x-ray absorption of the $SrAl_2O_4$ host matrix. The x-ray fluorescence yield was detected with a 9-element monolithic Ge detector[19]. Determination of the edge position, background subtraction and normalization of the calibrated raw XANES data was performed using Athena[20].

III. Results

A. Radioluminescence

When exposing the thermally emptied $SrAl_2O_4$:Eu,Dy phosphor to the x-ray beam, the sample starts to emit the characteristic bluish-green emission originating from the Eu^{2+} centers. In contrast to other Eu^{2+} doped phosphors which do not show a strong afterglow, the radioluminescence intensity does not immediately reach a constant value. Instead, the radioluminescence intensity monotonically increases until reaching a stationary value, which is shown in Fig. 2. The shape of the RL intensity curve is very similar to one for the photoluminescence intensity upon excitation with ultraviolet or blue light. This characteristic charging behavior is due to the competition between the fast photoluminescence process and the energy storage, i.e. the occupation of trap states [21]. Furthermore, we also verified that when heating the x-ray irradiated samples, a clear afterglow could be observed, confirming that thermally emptied persistent phosphors are charged by x-rays.

Figure 2 shows that the RL intensity increases rapidly and continues to grow until a stationary regime is reached after approximately two minutes. At this moment, the maximum number of charge traps is filled. The measurement temperature of 120K is sufficiently low to keep all trap levels filled due to the lack of thermal energy to induce the recombination process leading to the afterglow. The time evolution of the RL intensity, $I_{\mathrm{RL}}(t)$, can be expressed as a function of the final $I_{\mathrm{RL,\,f}}$ when all traps are filled and the RL intensity reaches a constant value:

$$I_{\mathrm{RL}}(t) = I_{\mathrm{RL,\,f}}\,(1 - F(t))$$

$F(t)$, as derived from the RL intensity profile, is shown in Fig. 3. It describes how many excitations in the phosphor are not used for (radio)luminescence, but instead lead to the filling of trap states. It can be approximated by two exponentially decaying components, so that

$$F(t) = A_1 e^{-t/\tau_1} + A_2 e^{-t/\tau_2}$$

The origin of these two components it not clear at this moment, but could be related to two different types of trap centers. Fitting $F(t)$ to the trap filling profile yields values of 7 and 42s for α_1 and α_2. Then the total number n of trapped charge carriers at a given time t_1 is proportional to

$$n(t_1) \approx \int_0^{t_1} \left(A_1 e^{-t/\tau_1} + A_2 e^{-t/\tau_2}\right) dt = \tau_1 A_1 \left(1 - e^{-t_1/\tau_1}\right) + \tau_2 A_2 \left(1 - e^{-t_1/\tau_2}\right)$$

This is only valid on condition that i) there is no thermal emptying of traps during the illumination and ii) no fading, tunneling or other non-radiative recombination occurs. The former is warranted by the low measurement temperature, while the latter losses are presumed negligible due to the short time scale of the measurements, certainly in comparison to the strong and long-lasting afterglow of $SrAl_2O_4$:Eu,Dy. The time dependency of $n(t_1)$ is shown in Fig. 3. After sufficiently long illumination (i.e. $t_1 \gg \tau_1, \tau_2$) all traps are filled and we find

$$n(t_1 \gg \tau_1, \tau_2) = n_f = \tau_1 A_1 + \tau_2 A_2$$

From the trap filling profile in Fig.3 we can derive that half of the traps are filled after only 15 seconds of x-ray illumination. After 80 seconds, 90% of all available traps are filled. This has important implications if one wants to use x-ray absorption techniques for studying the charge carrier dynamics in persistent phosphors, as will be discussed below. In addition, it was found that subsequent cycles of heating, cooling and X-ray irradiation have no influence on the shape or dimensions of the charging curve (inset on Fig. 2), indicating the absence of radiation damage of the material due to X-rays.

The RL emission spectrum at 120K under X-ray irradiation is essentially the same as under UV excitation, showing two broad Eu^{2+}-based bands, originating from Eu ions on the two different Sr-sites in the monoclinic host lattice (Fig. 4). The larger band is centered at 525nm and leads to the characteristic bright green color. A smaller band is located at 450nm and is only present at low temperatures [22]. In addition, Dy^{3+} emission originating from internal 4f-4f transitions is observed around 470nm, 570nm and 660nm. Dy^{3+} emission is only observed in RL and does not appear in photoluminescence, at least not upon excitation below the band gap (Fig. 4). Note that no emission from Eu^{3+}, which is characterized by its main emission lines around 595 to 615nm, could be detected, either in PL or upon x-ray irradiation.

After the discussion above on the luminescence behavior of the $SrAl_2O_4$:Eu,Dy persistent phosphor upon x-ray irradiation, we now focus on the x-ray absorption results, before merging both sets of observations.

B. XANES

The Eu L_{III} XANES spectra have a strong absorption line at the absorption edge due to $2p_{3/2} \rightarrow 5d$ electronic transitions. The spectra in Fig. 5 display the XANES spectra of $SrAl_2O_4$:Eu,Dy and the reference compounds. In the spectrum of $SrAl_2O_4$:Eu,Dy two well resolved edge resonances are visible, indicating two valence states for the Eu ions. The divalent and trivalent valence state can easily be distinguished since their edge resonances have different threshold energies [23]. The resonance for the Eu^{2+} is approximately 8 eV below the Eu^{3+} edge, which is compatible with the reference compounds of Eu^{2+} and Eu^{3+} (Fig. 5). The reason for this energy difference is the lower binding energy of the core electrons in Eu^{2+} caused by the shielding of the nucleus by the additional 4f electron. These spectra were analyzed by fitting procedures in which the white line transitions are approximated with pseudo-Voight curves and the absorption step by an arctangent function[24,25], to determine the peak area ratio between Eu^{3+} and Eu^{2+} as a function of x-ray irradiation time (Fig. 6).

The XANES spectra shown in Fig. 5 were collected with the monochromator scanning slowly through the entire spectrum, with a total collection time of typically one hour. By the time the interesting region for determining the valence state of Eu is reached (i.e. the white line transitions), all traps have already been filled, as was derived from the RL intensity profile. As we would like to differentiate between the states with empty and filled traps, fast scans of the XANES region were performed to measure the absorption edge within seconds after opening the x-ray beam. Unfortunately, this comes at the expense of spectral quality and a strongly decreased signal-to-noise ratio. About 130 short measurements were taken, with varying exposure time to the x-ray beam after the thermally emptying of all traps. The left panel of figure 6 shows the averaged spectrum obtained for all measurements started within 10s after opening the x-ray beam and for those after 120s of x-ray exposure, taken under identical conditions. The influence of the x-ray exposure is clearly seen, as the absorption peak related to Eu^{2+} decreases and the one for Eu^{3+} increases. Although it is obvious the fraction of europium ions changing their valence state during the charging process is small, the spectral changes can clearly be related to a valence state change by comparison to the peak positions of the reference samples with trivalent and divalent europium (Fig. 5). For the dysprosium co-dopant, no valence state changes are observed (Fig. 6) when comparing the XANES spectra before and after filling all traps.

To study the dynamics of the valence state change of Eu in more detail, the x-ray absorption peak area ratio between Eu^{3+} and Eu^{2+} was calculated for all the short XANES measurements separately and

plotted as a function of x-ray exposure (Fig. 7). As mentioned, the low signal-to-noise ratio leads to large scatter on the data points. First, the hypothesis of having a constant ratio was evaluated. In Fig. 7, the average peak ratio for all data points with $t > 85s$ was calculated, along with the standard deviation σ. Despite of the large scatter on the data points, the peak area ratios for the measurements with the shortest x-ray exposure time are well below this average, even when taking the large variability in the position of the data points into account (see inset of Fig. 7). Hence, the change in peak area ratio, or alternatively, the change in valence state for a fraction of the Eu ions, can be confirmed.

Now that we have established the valence state change for part of the Eu ions upon x-ray illumination, or equivalently, upon charging the persistent phosphor, we can verify whether the XANES data are compatible with the charging curve observed in the RL intensity, and the associated filling of traps. In our case, where the amount of Eu^{3+} is low compared to the amount of Eu^{2+}, we can approximate the change in the ratio $P_R(t)$ between the XANES peak area of Eu^{3+} and the one for Eu^{2+} as

$$P_R(t) \cong P_0 + c\frac{n(t)}{n_f}$$

In this equation, P_0 is related to the fraction of Eu^{3+} which is present in the material, irrespective of the fraction of filled traps. This can originate from the specific reducing conditions during the synthesis, and its presence is not uncommon in intentionally Eu^{2+}-doped phosphors. Also, it is possible some very deep traps are present in the phosphors, which were not emptied during the heating step in between all measurements. The parameters P_0 and c were fit to the XANES peak area ratios in Fig. 7, and values of 0.086 and 0.041 were obtained, respectively. The peak area ratios derived from the averaged XANES spectra after 10s and 120s of exposure to the x-ray beam (Fig. 6) are calculated at 0.105 (+/-0.005) and 0.130 (+/-0.005), respectively. These values are compatible with the peak area ratios derived for the individual XANES measurements in similar time windows (Fig.7), despite the large spread on the data points due to the short data acquisition time for each separate XANES measurement. Also, the fitted peak area ratio curve $P_R(t)$ through all data points in Fig. 7 yields values of $P_R(10\mathrm{s}) = 0.102$ and $P_R(120\mathrm{s}) = 0.126$, being in line with the values obtained from the averaged XANES spectra. It is obvious that the scatter on the data points does not allow to state confidently that the change in peak area ratio follows exactly the filling behavior of the traps. Nevertheless, the time-dependent variation in the peak area ratio is at least compatible with the time-dependency for the filling of the traps, as observed by monitoring the saturation behavior of the RL intensity.

IV. Discussion

The results show a relative increase in the peak area of the Eu^{3+} ions of about 4% with increasing irradiation time (or, equivalently, with increasing irradiation dose) for thermally emptied $SrAl_2O_4$:Eu,Dy upon exposure to x-rays. This indicates a change in valence state of a fraction of Eu-ions in the same order of magnitude[13]. Taking into account that the total number of europium ions in the material remains constant, and no monovalent[2] or tetravalent europium was observed at any time (energetically, this would be highly unlikely[11]), we can conclude that a part of the europium ions in the material undergoes a valence state change from divalent to trivalent during the charging by X-ray radiation. This confirms the ionization of Eu^{2+} to Eu^{3+} with liberation of an electron, which is suggested by various theoretical models of persistent luminescence[11-13]. Such an oxidation has previously been observed by Carlson *et al.* in $Sr_2MgSi_2O_7$:Eu^{2+},R^{3+} under high X-ray fluxes[5], but not by Qi *et al.*[26]. No

change in Eu^{3+}/Eu^{2+} ratio was detected in $CaAl_2O_4:Eu^{2+},R^{3+}$ nor $SrAl_2O_4:Eu^{2+},R^{3+}$, leading to the conclusion that no Eu^{3+} could be involved in the trapping process[6,27]. Rather, the formation of a Eu^{2+}-hole (h^+) pair seemed more plausible. Our results show that, despite these previous observations, there is ionization of Eu^{2+} to Eu^{3+} during charging. However, the ionization can only be observed on a short time scale, due to the high x-ray flux which almost immediately charges the phosphor. The measured amount of Eu^{2+} being ionized is in line with what can be expected on the basis of photometric measurements of the afterglow intensity after controlled excitation. Rodrigues et al. noted for $BaAl_2O_4$:Eu,Dy the possibility that the oxidation of Eu was caused by irreversible degradation of the phosphor by the X-ray irradiation[28], but the reproducibility of our observations during several experimental cycles show that this is unlikely and that the ionization must be related to the persistent luminescence.

The electrons liberated during the ionization of Eu^{2+} to Eu^{3+} are probably the charge carriers which are trapped during the charging process, as suggested by most of the theoretical models[11-13]. As mentioned earlier, some of these models predict the capture of the charge carriers by the codopant ions, resulting in a valence state change of the latter[1,11]. Our XANES measurements at the Dy-L_{III} edge, however, show that only Dy^{3+} is present in the material, independent of the duration of irradiation (Fig. 6). No Dy^{2+} or Dy^{4+} was observed at any point of the charging process. It seems that the electrons are trapped by defects in the host material (possibly vacancies), rather than by the codopant itself. The existence of such vacancies has been confirmed in $CaAl_2O_4$ by electron paramagnetic resonance (EPR) measurements [7]. Another possibility is the formation of a Dy^{3+}-electron pair, which would cause the electron to be trapped without an actual reduction of the codopant ion. Also, it is possible that reduction of the Dy^{3+} takes places but only for a minor fraction of the codopant ions, remaining undetected by regular XANES measurements.

From the RL intensity profile and the valence state change for europium (Fig. 5), it is clear that the state of the persistent phosphors (emptied or filled traps) is strongly influenced by the x-ray irradiation. For $SrAl_2O_4$:Eu,Dy, which is one of the best persistent phosphors in terms of total afterglow intensity, almost all traps are filled in about one minute. Hence x-ray absorption techniques should only be used with sufficient care to study changes in the valence state of dopants in persistent phosphors, especially for phosphors with less trapping capacity. In situ monitoring of the radioluminescence behavior, as was performed in this work, is advisable to assess the influence of the x-ray beam on the charging of the persistent phosphor being studied.

One could argue that the formation of Eu^{3+} is a result from the x-ray radiation, and is not related to the charging process of persistent phosphors. However, we verified on other Eu^{2+}-doped non-persistent luminescent materials that no Eu^{3+} could be detected after x-ray irradiation. The XANES spectrum for SrS:Eu^{2+} (which does not show persistent luminescence) is shown as an example in Fig. 4, indicating only the presence of Eu^{2+}. Also, the EuS reference sample only shows Eu^{2+}, without any trace of Eu^{3+}.

Consequently, we can confidently state that an oxidation of a significant fraction of the Eu^{2+} ions to Eu^{3+} occurs during the charging of persistent phosphors. Furthermore, the valence state change appears to occur on the same time scale as the filling of the traps (Fig. 7). Despite the large scatter on the data points, this similar time dependency is a strong indication that this valence change is related to the charging mechanism itself.

Due to the (initially) fast charging of the persistent phosphor under x-ray irradiation and the minimal x-ray exposure time for the determination of the Eu^{3+}/Eu^{2+} ratio, it is not possible in the present setup to determine directly whether Eu^{3+} is already present in thermally emptied $SrAl_2O_4$:Eu,Dy, simply because in the used setup it is not possible to measure the XANES region on the sub second time scale.

Although the scatter on the XANES results (Fig. 7) does not allow extrapolating the valence ratio to time zero with sufficient accuracy, there is presumably some fraction of trivalent europium present at the start of the measurement. This could be due to (intrinsic) Eu^{2+} ions which were previously ionized and for which the heating prior to the x-ray irradiation was not sufficient to release the trapped electron. Also it is possible that a certain amount of Eu^{3+} is present in the material, irrespective of the illumination of the phosphor. The presence of both valence states Eu^{2+} and Eu^{3+} would not be surprising, taking into account the low reduction potential of europium[29]. Even though the dopant and codopant are usually added to the host crystal in their trivalent state (R_2O_3 or RF_3 being the most common choices), the reductive atmosphere under which the samples are prepared is able to reduce most of the Eu. However, the present XANES results show that this reduction is possibly not complete. For dysprosium, the reduction potential is about 2eV higher[29], explaining why all codopant ions are in a trivalent state.

The combined radioluminescence and x-ray absorption observations are an important starting point for the construction of appropriate energy level schemes and structural models explaining the mechanism of persistent luminescence, preferably in a generic way for all Eu^{2+}-based phosphors [1]. During the charging of $SrAl_2O_4$:Eu,Dy an ionization of Eu^{2+} to Eu^{3+} clearly occurs, indicating that electrons are the relevant charge carriers, in contrast to several earlier models [1]. The electron is however not trapped onto Dy^{3+} to form Dy^{2+}, as the applied XANES experiments are considered to be sufficiently sensitive to detect the possible formation of Dy^{2+}. Hence, the model involving the electron capture by Dy^{3+}, as proposed by Dorenbos [11], seems not appropriate for $SrAl_2O_4$:Eu,Dy. Nevertheless this model based on the position of the rare earth's energy levels within the band gap has shown strong predictive character for the thermoluminescence behavior of Ln^{3+} doped phosphates, assuming the electron trapping by Ln^{3+} ions [30, 31]. The model by Clabau et al. [12], where the electron is trapped at a nearby defect (presumably an oxygen vacancy) is compatible with the XANES and RL results. In this model, the role of Dy^{3+} is a stabilization and deepening of the electron traps already present in $SrAl_2O_4$:Eu. To construct more quantitative energy level models, effects of (Coulomb) interaction between the ionized europium and the nearby trapped electron, along with relaxation effects, should be included [32].

V. Conclusions.

In conclusion, we have combined radioluminescence and x-ray absorption spectroscopy to study the valence states of europium and dysprosium ions in the persistent luminescent material $SrAl_2O_4$:Eu,Dy. During the charging/trapping process, part of the europium ions ionize from Eu^{2+} to Eu^{3+}, in contrast with previously reported x-ray absorption studies. However, no reduction of the Dy^{3+} ions could be detected, indicating that the released electrons are not captured by the codopant ions. These are important observations which should be included in future models for the mechanism of persistent luminescence.

Acknowledgments

This work is financially supported by the Dutch-Belgian Beamline project (DUBBLE) funded by the Netherlands Organisation for Scientific Research (NWO) and the Research Foundation Flanders (FWO), and by the UGent Special Research Fund (BOF). The authors would like to acknowledge Wim Bras for experimental support and useful discussions.

Fig. 1. The experimental set-up combining XANES and PL measurements.

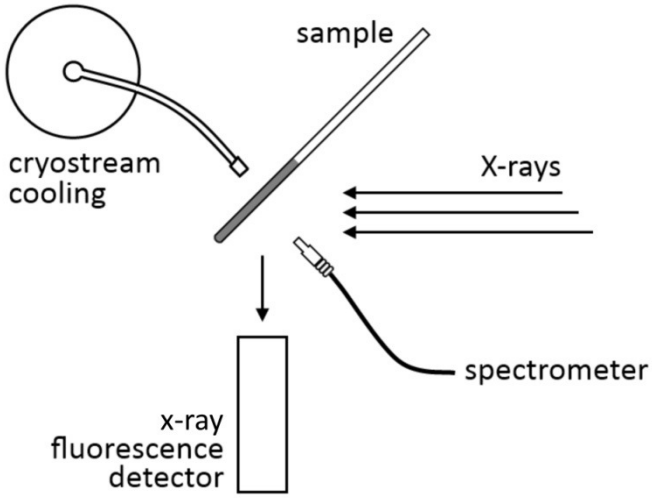

Fig. 2. Luminescence intensity of Sr_2AlO_4:Eu,Dy as a function of the x-ray irradiation time at 120K, after the sample was thermally emptied and kept in the dark prior to the irradiation.

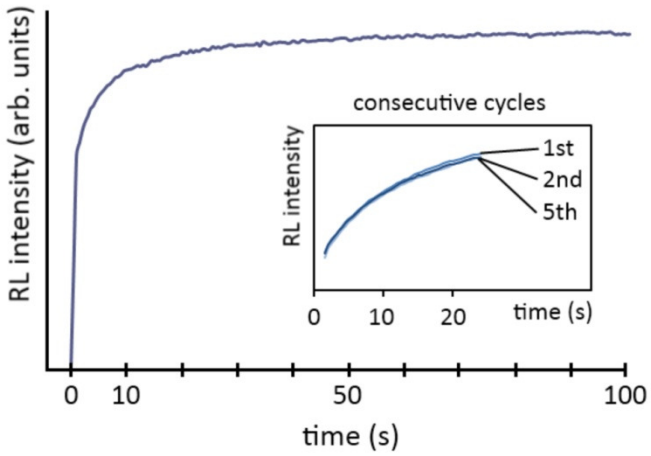

Fig. 3. Evolution of the trap filling rate $F(t)$ as a function of x-ray irradiation time at 120K, obtained from the RL intensity profile. Two exponentials (dotted lines) were fit to the experimental data points (red diamonds). The blue curve shows the fraction $n(t)/n_f$ of filled traps.

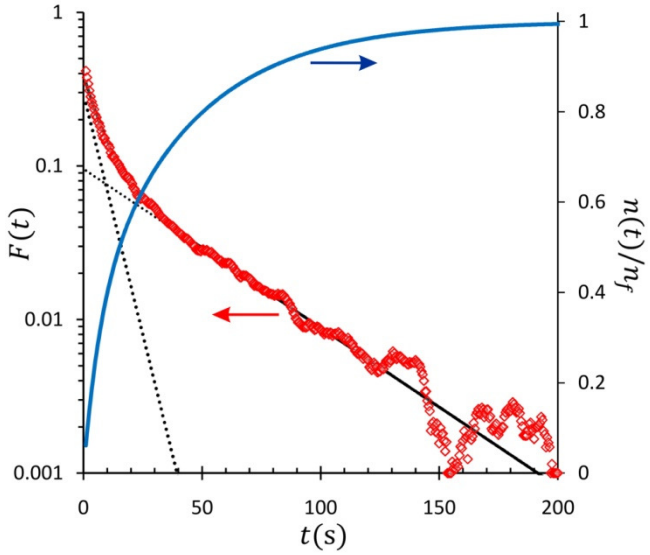

Fig. 4 **(a)** Radioluminescence spectrum of $SrAl_2O_4$:Eu,Dy at 120K, **(b)** Photoluminescence spectrum at 120K upon excitation at 365nm. The arrows indicate the positions of Dy^{3+} emission. The spectra are shifted vertically for clarity.

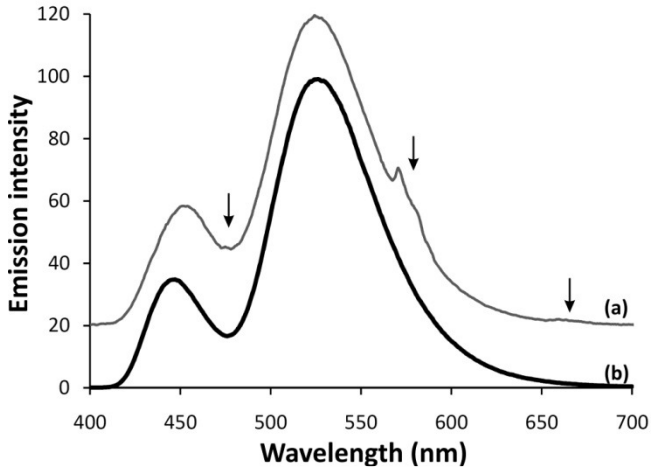

Fig. 5. Eu L_{III} XANES spectra of $SrAl_2O_4$:Eu,Dy at 120K and SrS:Eu. EuS and Eu_2O_3 were measured as reference compounds. Zero of the relative energy scale is set at the position of the Eu^{2+} resonance. The spectra are shifted vertically for clarity.

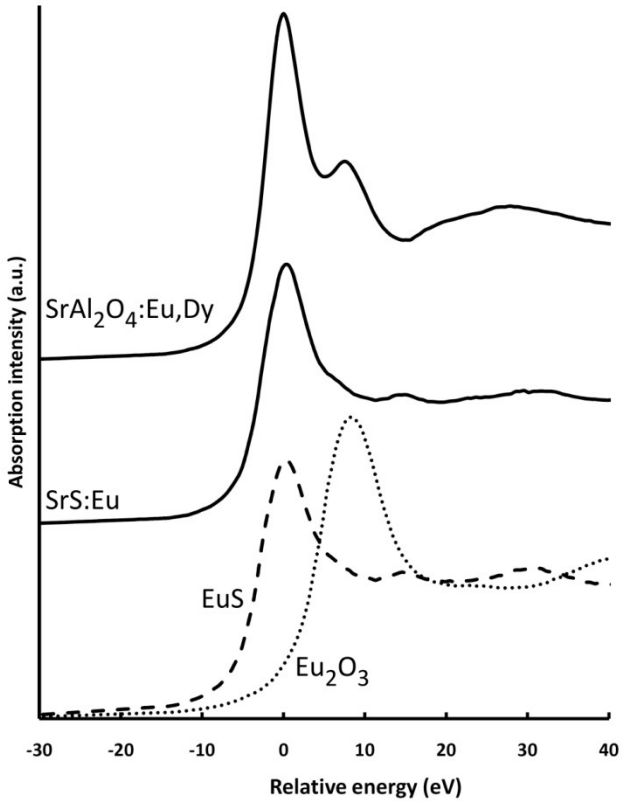

Fig. 6. Averaged XANES spectra for Eu (**left**) and Dy (**right**) in $SrAl_2O_4$:Eu,Dy at 120K started within 10 seconds (full line) and after 120 seconds (dotted line) of exposure to the x-ray beam. Reference positions for the divalent and trivalent Eu and Dy L_{III} edges are indicated.

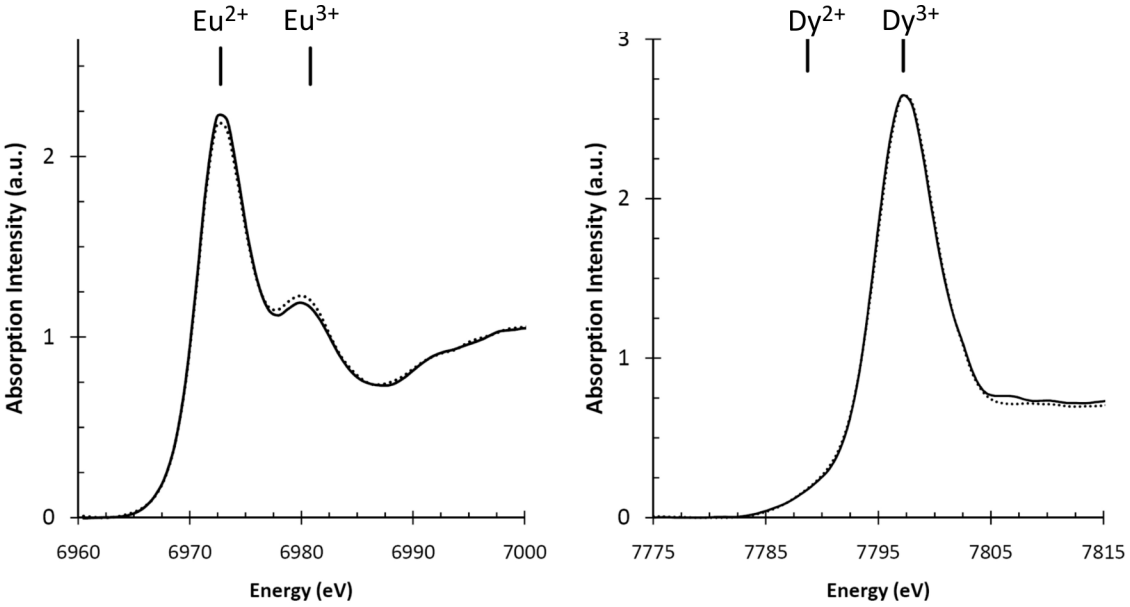

Fig. 7. XANES peak area ratio between Eu^{3+} and Eu^{2+} as a function of x-ray irradiation time at 120K, for all separate experiments (diamonds). The dashed line is the best fit assuming a constant ratio, based on all data points with $\boldsymbol{t} > 85s$, the dotted lines show the standard deviation ($\boldsymbol{\sigma}$). The full red line is a fitted line based on the number of trapped charges as derived from the RL data (see text for details). The bottom image shows an enlarged image for the first 40 seconds of x-ray exposure.

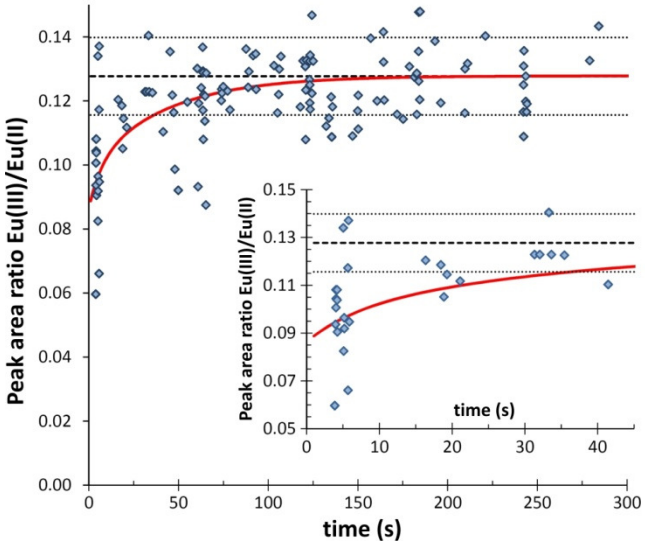

References

[1] K. Van den Eeckhout, P. F. Smet, and D. Poelman, Materials **3**, 2536 (2010).

[2] T. Matsuzawa, Y. Aoki, N. Takeuchi, and Y. Murayama, Journal of The Electrochemical Society **143**, 2670 (1996).

[3] Q. L. de Chermont, C. Chaneac, J. Seguin, F. Pelle, S. Maitrejean, J. P. Jolivet, D. Gourier, M. Bessodes, and D. Scherman, Proc. Natl. Acad. Sci. U. S. A. **104**, 9266 (2007).

[4] T. Maldiney, C. Richard, J. Seguin, N. Wattier, M. Bessodes, and D. Scherman, ACS Nano **5**, 854 (2011).

[5] S. Carlson, J. Hölsä, T. Laamanen, M. Lastusaari, M. Malkamäki, J. Niittykoski, and R. Valtonen, Optical Materials **31**, 1877 (2009).

[6] J. Holsa, T. Laamanen, M. Lastusaari, M. Malkamaki, E. Welter, and D. A. Zajac, Spectrochimica Acta Part B-Atomic Spectroscopy **65**, 301 (2010).

[7] J. Hölsä, T. Aitasalo, H. Jungner, M. Lastusaari, J. Niittykoski, and G. Spano, Journal of Alloys and Compounds **374**, 56 (2004).

[8] H. B. Yuan, W. Jia, S. A. Basun, L. Lu, R. S. Meltzer, and W. M. Yen, Journal of The Electrochemical Society **147**, 3154 (2000).

[9] A. J. J. Bos, R. M. van Duijvenvoorde, E. van der Kolk, W. Drozdowski, and P. Dorenbos, J. Lumines. **131**, 1465 (2011).

[10] T. Aitasalo, J. Hölsä, M. Kirm, T. Laamanen, M. Lastusaari, J. Niittykoski, J. Raud, and R. Valtonen, Radiation Measurements **42**, 644 (2007).

[11] P. Dorenbos, Journal of The Electrochemical Society **152**, H107 (2005).

[12] F. Clabau, X. Rocquefelte, S. Jobic, P. Deniard, M. H. Whangbo, A. Garcia, and T. Le Mercier, Chemistry of Materials **17**, 3904 (2005).

[13] T. Aitasalo, J. Hölsä, H. Jungner, M. Lastusaari, and J. Niittykoski, The Journal of Physical Chemistry B **110**, 4589 (2006).

[14] G. Moreau, L. Helm, J. Purans, and A. E. Merbach, Journal of Physical Chemistry A **106**, 3034 (2002).

[15] G. Moreau, R. Scopelliti, L. Helm, J. Purans, and A. E. Merbach, Journal of Physical Chemistry A **106**, 9612 (2002).

[16] R. M. Martin, J. B. Boyce, J. W. Allen, and F. Holtzberg, Phys. Rev. Lett. **44**, 1275 (1980).

[17] S. Nikitenko, A. M. Beale, A. M. J. van der Eerden, S. D. M. Jacques, O. Leynaud, M. G. O'Brien, D. Detollenaere, R. Kaptein, B. M. Weckhuysen, and W. Bras, Journal of Synchrotron Radiation **15**, 632 (2008).

[18] http://www.glotechint.com.

[19] G. Derbyshire, K. C. Cheung, P. Sangsingkeow, and S. S. Hasnain, Journal of Synchrotron Radiation **6**, 62 (1999).

[20] B. Ravel and M. Newville, Journal of Synchrotron Radiation **12**, 537 (2005).

[21] D. Jia, Optical Materials **22**, 65 (2003).

[22] F. C. Palilla, A. K. Levine, and M. R. Tomkus, Journal of The Electrochemical Society **115**, 642 (1968).

[23] G. Wortmann, Hyperfine Interact. **47-8**, 179 (1989).

[24] G. Silversmit, H. Poelman, V. Balcaen, P. M. Heynderickx, M. Olea, S. Nikitenko, W. Bras, P. F. Smet, D. Poelman, R. De Gryse, M. F. Reniers, and G. B. Marin, Journal of Physics and Chemistry of Solids **70**, 1274 (2009).

[25] Y. Takahashi, G. R. Kolonin, G. P. Shironosova, Kupriyanova, II, T. Uruga, and H. Shimizu, Mineralogical Magazine **69**, 179 (2005).

[26] Z. M. Qi, C. S. Shi, M. Liu, D. F. Zhou, X. X. Luo, J. Zhang, and Y. N. Xie, Physica Status Solidi a-Applied Research **201**, 3109 (2004).

[27] J. Qiu, M. Kawasaki, K. Tanaka, Y. Shimizugawa, and K. Hirao, Journal of Physics and Chemistry of Solids **59**, 1521 (1998).

[28] L. C. V. Rodrigues, R. Stefani, H. F. Brito, M. Felinto, J. Holsa, M. Lastusaari, T. Laamanen, and M. Malkamaki, Journal of Solid State Chemistry **183**, 2365 (2010).
[29] S. Cotton, *Lanthanide and actinide chemistry* (Wiley, Chichester, 2006).
[30] A. J. J. Bos, P. Dorenbos, A. Bessière, and B. Viana, Radiation Measurements **43**, 222 (2008).
[31] A. H. Krumpel, A. J. J. Bos, A. Bessiere, E. van der Kolk, and P. Dorenbos, Phys. Rev. B **80**, 085103 (2009).
[32] M. Grinberg, Journal of The Electrochemical Society **157**, G100 (2010).